Int. J. Heat Mass Transfer. Vol. 15, pp. 2133–2142. Pergamon Press 1972. Printed in Great Britain

EFFECTS OF FORCED FLOW, NONCONDENSABLES, AND VARIABLE PROPERTIES ON FILM CONDENSATION OF PURE AND BINARY VAPORS AT THE FORWARD STAGNATION POINT OF A HORIZONTAL CYLINDER*

V. E. DENNY and V. SOUTH III
University of California, Los Angeles, California 90024, U.S.A.

(*Received* 20 *August* 1971 *and in revised form* 7 *January* 1972)

Abstract—An analytical investigation of the effects of forced flow, noncondensable gas, and variable thermophysical properties on laminar film condensation of pure and binary vapors at the forward stagnation point of a horizontal cylinder is presented. Condensation heat transfer results are obtained for a broad range of parameters including the oncoming bulk velocity (u_∞ = 1–100 ft/s), saturation pressure (P_∞ = 49–760 Torr), wall-to-bulk temperature difference ($T_\infty - T_w$ = 0·3–40°F), mass fraction non-condensable gas ($m_{1,\infty}$ = 0·01–0·15), and cylinder radius (R = 0·25–1·5 in.). As expected, the deleterious effects of noncondensable gas on q/q_{Nu} (q_{Nu} is the classical Nusselt solution for pure vapor) under quiescent conditions are markedly less severe with forced flow. (For steam–air mixtures, with $0{\cdot}01 \leqslant m_{1,\infty} \leqslant 0{\cdot}15$, q/q_{Nu} approximately doubles as u_∞ increases from 1 to 10 ft/s.) As was true for the flat plate results of Minkowycz and Sparrow, q/q_{Nu} passes through a maximum as $T_\infty - T_w$ increases; here, the maxima occur at higher $T_\infty - T_w$ and are more pronounced. For binary film condensation of steam–methanol mixtures, it is found that q/q_{Nu} (q_{Nu} is the classical Nusselt solution for pure steam) sharply decreases with increasing bulk concentration of (more volatile) methanol; the effect is similar to that for noncondensable gas. Guided by the numerical results, a simplified theory is developed which is in good agreement with the heat and mass transfer conductances.

NOMENCLATURE

A, physical property group $= k_l^3\rho_l\lambda/\nu_l$;
$\mathscr{B}$, mass transfer driving force;
C_p, heat capacity;
$\mathscr{D}_{12}$, binary diffusion coefficient;
f, dimensionless stream function;
Fr, Froude number $= gR/4u_\infty^2$;
g, acceleration of gravity;
$\mathscr{g}$, mass-transfer conductance;
j, mass diffusion flux;
k, thermal conductivity;
m, mass fraction;
$\dot{m}$, interfacial mass flux $= \rho v|_s$;
p, partial pressure;
P, total pressure;
Pr, Prandtl number $= \mu C_p/k$;
q, heat flux;
q_{Nu}, Nusselt heat flux;
R, cylinder radius;
Re, Reynolds number $= 2Ru_\infty/\nu_\infty$;
Sc, Schmidt number $= \nu/\mathscr{D}_{12}$;
T, absolute temperature;
u, v, velocity components;
x, y, boundary-layer coordinates.

Greek symbols
δ, liquid film thickness;
η, similarity variable $= Re^{\frac{1}{2}}y/R$;
λ, latent heat of vaporization;
μ, viscosity;
ν, kinematic viscosity;

* This work was supported by the Department of the Interior, OSW Grant No. 14-30-2678. Computer time for the numerical calculations was provided in part by the Campus Computing Network of the University of California, Los Angeles.

ρ, density;
τ, shear stress;
ϕ_μ, viscosity ratio $= \mu_v/\mu_\infty$;
ϕ_ρ, density ratio $= \rho_v/\rho_\infty$.

Subscripts
e, at the vapor boundary-layer edge;
i, at the vapor–liquid interface;
l, in the liquid phase;
s, at the s-surface (Fig. 1);
u, at the u-surface (Fig. 1);
v, in the vapor phase;
w, at the wall;
0, as $\dot{m} \to 0$;
-1, as $\mathscr{B} \to -1$;
1, of the more volatile species;
2, of the less volatile species;
∞, at infinity.

INTRODUCTION

BEGINNING with the classical analysis of Nusselt in 1916 [1], film condensation on a horizontal cylinder has been a subject of active analytical study. Bromley [2] and Rohsenow [3] extended Nusselt's analysis to include sensible heat effects in the liquid film. Sparrow and Gregg [4] considered boundary-layer forms of the conservation equations for the film and employed an approximate similarity transformation to obtain solutions for pure vapors assuming constant properties and neglecting vapor drag. Shekriladze and Gomelauri [5] invoked Nusselt's assumptions, whereby the effects of liquid acceleration and energy convection are neglected, and obtained an analytical solution for the case of forced flow of a saturated vapor at zero gravity. Denny and Mills [6] extended the analysis of [5] to obtain solutions at normal gravity. In addition, they demonstrated that negligible error is incurred, for all but low Prandtl number fluids, on invoking the Nusselt assumptions and evaluating locally variable properties by means of the reference temperature concept.

Since the usual industrial situation involves film condensation under partial vacuum, the vapor phase invariably contains small amounts of noncondensable gas. As demonstrated by Minkowycz and Sparrow [7] for a quiescent vapor condensing on a vertical plate, this results in marked reductions in heat-transfer rates. As shown in [8], these effects are less severe under conditions of forced flow.

At present, no systematic investigation of the effects of noncondensable gas on film condensation of pure vapors undergoing forced flow over a horizontal cylinder has appeared. Although Othmer [9] has investigated experimentally the problem for steam–air mixtures, results were obtained only for overall rates of heat transfer and the convective situation in the vapor phase was uncertain. For film condensation of mixed vapors, no work, to the authors' knowledge, has appeared; although Sparrow and Marschall [10] have examined binary, gravity flow film condensation of a quiescent vapor on a vertical flat plate.

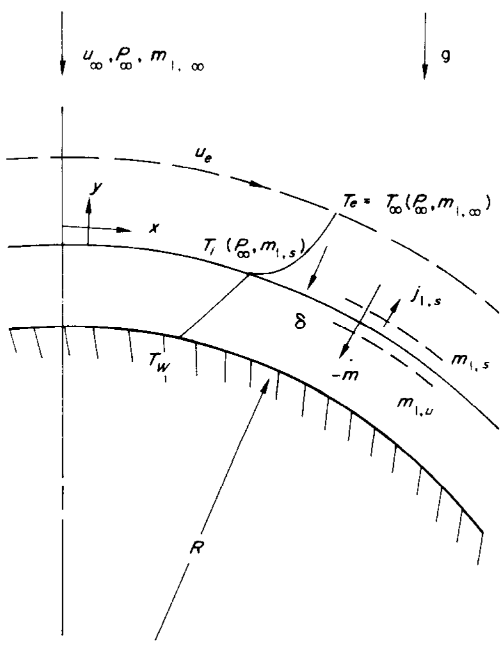

FIG. 1. Schematic of physical situation.

This investigation is concerned with laminar film condensation of a pure vapor in the presence of a noncondensable gas, as well as with condensation of a binary mixture, at the upper stagnation point of a horizontal cylinder (Fig. 1). The oncoming vapor is assumed to flow laminarly downwards over the cylinder under conditions for which a thin boundary layer forms near $x = 0$. At great distance from the surface, the vapor has velocity u_∞, temperature T_∞, and mass fraction of the more volatile species $m_{1,\infty}$. The system pressure P_∞ is determined from T_∞ and $m_{1,\infty}$, assuming the vapor to be saturated. At the vapor–liquid interface, the compositions $m_{1,s}$ and $m_{1,u}$ are determined by P_∞ and T_i, assuming thermodynamic equilibrium applies. The condensate film has thickness δ, which may be taken to be constant in the stagnation region.

The objectives of the paper are two-fold. First, a rigorous theory is formulated which is based on the conservation laws and related physicochemical principles. The resulting theory is applied to film condensation of steam from steam–air mixtures and to binary film condensation of steam–methanol mixtures. Guided by the results of the rigorous analysis, a semi-empirical theory is developed which provides a convenient basis for engineering calculations.

ANALYSIS

Governing equations

Paralleling arguments in [8] and [11], the governing equations are taken as

$$\frac{\partial}{\partial x}(\rho_v u) + \frac{\partial}{\partial y}(\rho_v v) = 0 \tag{1}$$

$$\rho_v u \frac{\partial u}{\partial x} + \rho_v v \frac{\partial u}{\partial y} = \frac{\partial}{\partial y}\left(\mu_v \frac{\partial u}{\partial y}\right) + \rho_v g \sin\frac{x}{R} - \frac{\mathrm{d}P}{\mathrm{d}x} \tag{2}$$

$$\rho_v u \frac{\partial m_1}{\partial x} + \rho_v v \frac{\partial m_1}{\partial y} = \frac{\partial}{\partial y}\left(\frac{\mu_v}{Sc}\frac{\partial m_1}{\partial y}\right) \tag{3}$$

$$\rho_v u \frac{\partial T}{\partial x} + \rho_v v \frac{\partial T}{\partial y} = \frac{\partial}{\partial y}\left(\frac{\mu_v}{Pr}\frac{\partial T}{\partial y}\right) + \frac{\mu_v}{Pr}\frac{\partial T}{\partial y}\left[\frac{\partial \ln C_{p,v}}{\partial y} + \frac{Pr}{Sc}\frac{C_{p,1} - C_{p,2}}{C_{p,v}}\frac{\partial m_1}{\partial y}\right] \tag{4}$$

for the vapor boundary layer and

$$\mathrm{d}^2u/\mathrm{d}y^2 = -[\rho_l g \sin(x/R) - \mathrm{d}P/\mathrm{d}x]/\mu_l \tag{5}$$

$$\mathrm{d}^2m_1/\mathrm{d}y^2 = \mathrm{d}^2T/\mathrm{d}y^2 = 0 \qquad (6), (7)$$

for the liquid film. Neglecting second order effects of non-uniform suction [12], the static pressure gradient is taken as

$$-\mathrm{d}P/\mathrm{d}x = [(4\rho_\infty u_\infty^2/R)\cos(x/R) - \rho_\infty g]\sin(x/R). \tag{8}$$

Equations (1)–(7) are subject to the boundary conditions

$$u \to u_e \equiv 2u_\infty \sin(x/R), \quad m_1 \to m_{1,\infty}, \quad \text{and } T \to T_\infty \tag{9}$$

at the "edge" of the vapor boundary layer;

$$u = 0, \quad \mathrm{d}m_1/\mathrm{d}y = 0, \quad \text{and } T = T_w \tag{10}$$

at the surface of the cylinder; and

$$u|_u = u|_s = u_i \tag{11}$$

$$\mu_l\, \partial u/\partial y|_u = \mu_v\, \partial u/\partial y|_s = \tau_i \tag{12}$$

$$\dot{m}m_1|_u = \dot{m}m_1|_s + j_{1,y}|_s = \dot{m}m_1|_s - \rho_v \mathscr{D}_{12}\, \partial m_1/\partial y|_s \tag{13}$$

$$m_{1,u} = m_{1,u}(m_{1,s}, P_\infty) \tag{14}$$

$$T|_u = T|_s = T_i(m_{1,s}, P_\infty) \tag{15}$$

$$k_l\, \partial T/\partial y|_u = -\dot{m}\lambda + k_v\, \partial T/\partial y|_s \tag{16}$$

at the vapor–liquid interface. In equations (14) and (15), thermodynamic equilibrium is assumed to apply, with $m_{1,u} = 0$ when the more volatile component is "noncondensable". The interfacial mass flux is given by

$$\rho_v v|_s \equiv \dot{m} = -\mathrm{d}/\mathrm{d}x \int_0^\delta \rho u\, \mathrm{d}y\Big|_l \tag{17}$$

where δ is the liquid film thickness.

Method of solution

Introducing the similarity variable $\eta = Re^{\frac{1}{2}}y/R$ and stream function $\psi = \rho_\infty u_e Rf/Re^{\frac{1}{2}}$, equations (1)–(4) reduce to

$$[\phi_u(f'/\phi_\rho)']' + f(f'/\phi_\rho)' = -[1 - \phi_\rho(f'/\phi_\rho)^2 + Fr(\phi_\rho - 1)] \quad (18)$$

$$(\phi_\mu m_1'/Sc)' + fm_1' = 0 \quad (19)$$

$$(\phi_\mu T'/Pr)' + fT' = -(\phi_\mu T'/Pr)\,[C'_{p,v} + Pr(C_{p,1} - C_{p,2})\,.\,m_1'/Sc]/C_{p,v} \quad (20)$$

where $f'/\phi_\rho \equiv u/u_e$; primes denote differentiation with respect to η; and $\phi_\rho = \rho_v/\rho_\infty$, $\phi_\mu = \mu_v/\mu_\infty$, $Re = 2Ru_\infty/v_\infty$, $Fr = gR/4u_\infty^2$, $Sc = v_v/\mathscr{D}_{12}$, and $Pr = \mu_v C_{p,v}/k_v$. The boundary conditions, equations (9) and (11)–(16), become

$$f'/\phi_\rho \to 1, \quad m_1 \to m_{1,\infty}, \quad \text{and } T \to T_\infty \quad (21)$$

at $\eta = \eta_e$ and, in view of equations (5)–(7) and (10),

$$f'/\phi_\rho = u_i/u_e = (\mu_\infty/\mu_l)\,[(Fr(\rho_l/\rho_\infty - 1) + 1)(\delta^*/2) + \phi_\mu(f'/\phi_\rho)']\,\delta^* \quad (22)$$

$$f = k_l(T_i - T_w)/\mu_\infty\lambda\delta^* - (C_{p,v}/\lambda)\,.\,\phi_\mu T'/Pr \quad (23)$$

$$\phi_\mu m_1'/Sc = f\,.\,(m_{1,u} - m_{1,s}) \quad (24)$$

$$T_i = T_i(m_{1,s}, P_\infty) \quad (25)$$

at $\eta = 0$. For binary condensation, $\lambda = m_{1,u}\lambda_1 + m_{2,u}\lambda_2$ with, of course, $m_{1,u} = m_{1,u}(m_{1,s}, P_\infty)$.

Equations (18)–(20) were recast in integral form and solved iteratively, the dimensionless film thickness $\delta^* \equiv Re^{\frac{1}{2}}\delta/R$ appearing in equations (22) and (23) being extracted from simultaneous solution of equations (16) and (17). Variable thermophysical properties were calculated as outlined in [11].

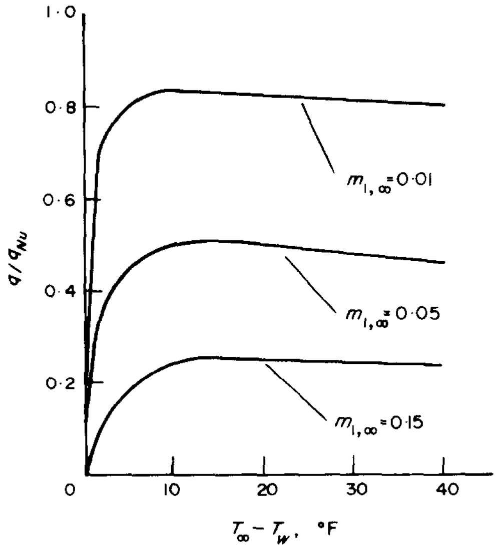

FIG. 2. Effects of $T_\infty - T_w$ and $m_{1,\infty}$ on condensation heat transfer for steam–air: $P_\infty = 760$ Torr, $u_\infty = 1$ ft/s, $R = 0{\cdot}75$ in.

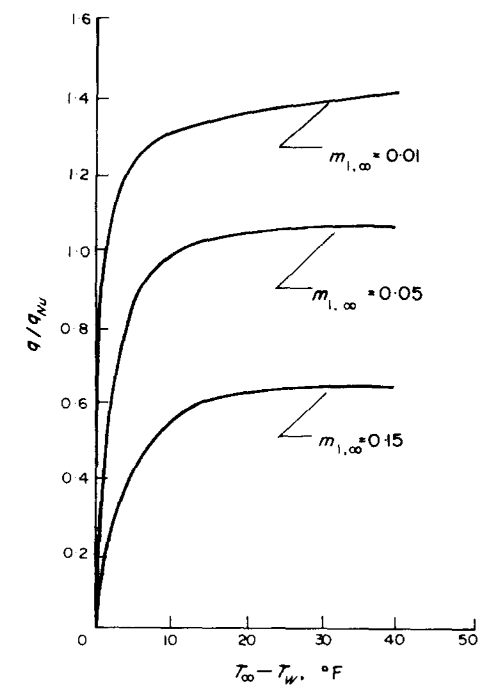

FIG. 3. Effects of $T_\infty - T_w$ and $m_{1,\infty}$ on condensation heat transfer for steam–air: $P_\infty = 760$ Torr, $u_\infty = 10$ ft/s, $R = 0{\cdot}75$ in.

RESULTS AND DISCUSSION

Typical results for stagnation-point heat transfer from saturated vapor mixtures undergoing forced flow over a horizontal cylinder are presented in Figs. 2–7, where q_{Nu} is the classical

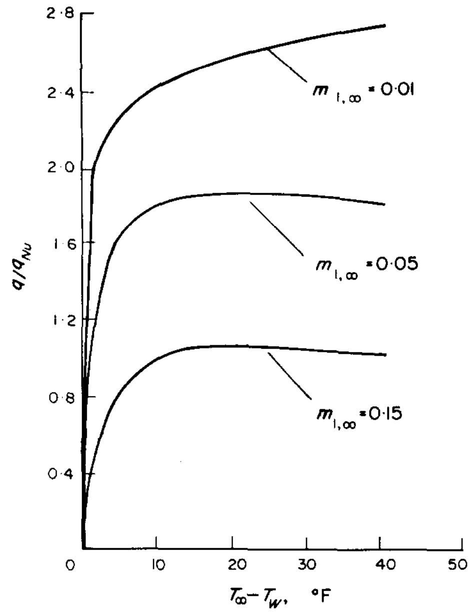

FIG. 4. Effects of $T_\infty - T_w$ and $m_{1,\infty}$ on condensation heat transfer for steam–air: $P_\infty = 49$ Torr, $u_\infty = 100$ ft/s, $R = 0{\cdot}75$ in.

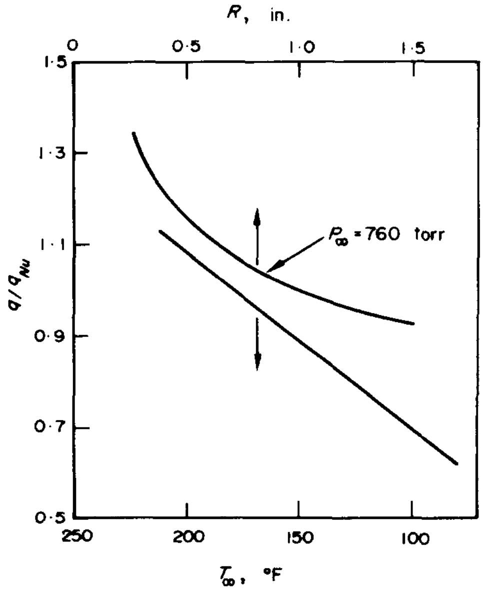

FIG. 5. Effects of R and T_∞ on condensation heat transfer for steam–air: $u_\infty = 10$ ft/s, $T_\infty - T_w = 20$°F, $m_{1,\infty} = 0{\cdot}05$.

Nusselt result [1] for pure steam based on $(T_\infty - T_w)$ and neglecting vapor drag. To first order, the results are characterized by the effects of the problem parameters ($T_\infty - T_w$, $m_{1,\infty}$, u_∞, T_∞ and R) on the mass-transfer conductance g. From equation (13),

$$\dot{m} = \frac{m_{2,\infty} - m_{2,s}}{m_{2,s} - m_{2,u}} \cdot \rho \mathscr{D}_{12} \frac{\partial}{\partial y}\left(\frac{m_2}{m_{2,\infty} - m_{2,s}}\right) = \mathscr{B} \cdot g \qquad (26)$$

where, as discussed in [8], $\mathscr{B} \to -1$ as $\dot{m} \to -\infty (m_{2,\infty} \to 1)$. In the $\mathscr{B} \to -1$ limit,

$$g_{-1} = 2\rho_\infty u_\infty Re^{-\frac{1}{2}} Sc_\infty^{-\frac{1}{2}}/[(1 + Sc_\infty)(1 + \mathscr{B})]^{\frac{1}{2}} \qquad (27)$$

as shown by Acrivos [13]. Since μ_∞ and Sc_∞ are weakly dependent on $m_{1,\infty}$ and T_∞ for the systems considered here,

$$g_{-1} \propto (\rho_\infty u_\infty)^{\frac{1}{2}} R^{-\frac{1}{2}}/(1 + \mathscr{B})^{\frac{1}{2}}.$$

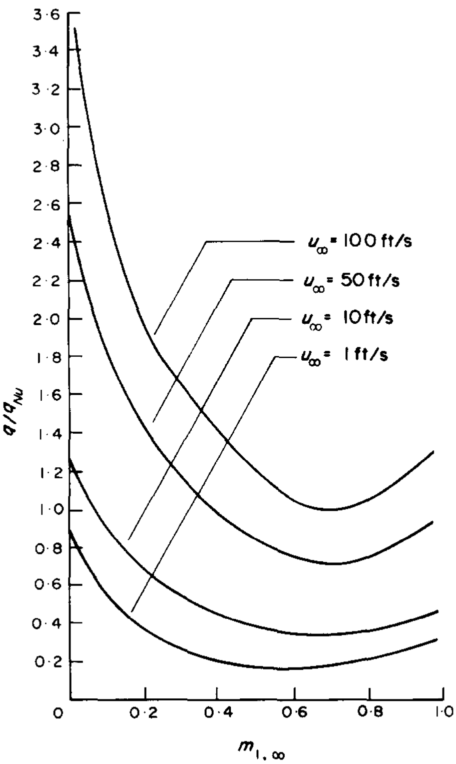

FIG. 6. Effects of u_∞ and $m_{1,\infty}$ on condensation heat transfer for steam–methanol: $P_\infty = 760$ Torr, $T_\infty - T_w = 20$°F, $R = 0{\cdot}75$ in.

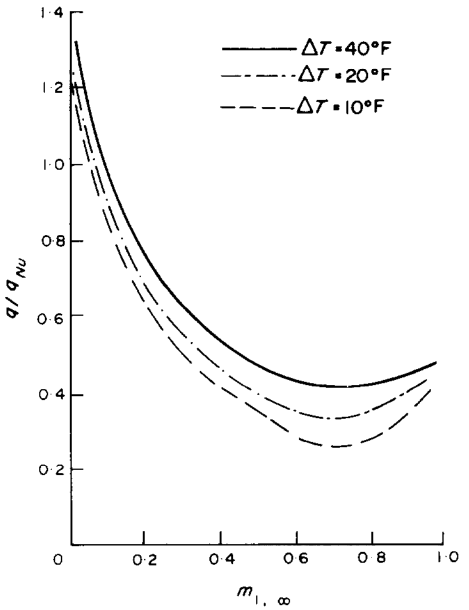

FIG. 7. Effects of $T_\infty - T_w$ and $m_{1,\infty}$ on condensation heat transfer for steam–methanol: $P_\infty = 760$ Torr, $u_\infty = 10$ ft/s, $R = 0{\cdot}75$ in.

Observing further that

$$q_{Nu} \propto (k_l^3\rho_l^2\lambda/\mu_l)^{\frac{1}{4}}(T_\infty - T_w)^{\frac{3}{4}} = A_0^{\frac{1}{4}}(T_\infty - T_w)^{\frac{3}{4}},$$

$$q/q_{Nu} \propto (\rho_\infty u_\infty)^{\frac{1}{2}}R^{-\frac{1}{2}}|\mathscr{B}|/[(1+\mathscr{B})^{\frac{1}{2}} \times A_0^{\frac{1}{4}}\cdot(T_\infty - T_w)^{\frac{3}{4}}]. \quad (28)$$

Applying equation (28) and referring to Table 1 for appropriate values of problem parameters, interpretation of the trends in Figs. 2–7 is now straightforward.

Steam (m_2)–*air* (m_1) *results*

For given $T_\infty - T_w$, q/q_{Nu} increases (Figs. 2–4) with increasing $(\rho_\infty u_\infty)^{\frac{1}{2}}$ and $|\mathscr{B}|$ and decreases (Fig. 5) with decreasing P_∞ (i.e. ρ_∞) and increasing R, as suggested by equation (28). (The results at $P_\infty = 49$ Torr (Fig. 4) are atypically high because q_{Nu} is appreciably reduced via significantly larger values of μ_l at the lower film temperatures.) The effects of $T_\infty - T_w$ on q/q_{Nu} are less straightforward. As $(T_\infty - T_w) \to 0$, $q/q_{Nu} \to 0$ as well since $q \propto (T_i - T_w)^{\frac{3}{4}}$ and $(T_i - T_w) < (T_\infty - T_w)$ for $(T_\infty - T_w)$ arbitrarily small. Furthermore, q/q_{Nu} must approach zero as $(T_\infty - T_w) \to \infty$ since q is bounded by the asymptotic limit on $\mathscr{B} = (m_{2,\infty} - m_{2,s})/(m_{2,s} - 1) \to -m_{2,\infty}$. Thus, maxima in the curves for q/q_{Nu} vs. $(T_\infty - T_w)$ occur. Their precise location is, of course, a complex function of the problem parameters; in principle, they could be extracted from equation (28), obtaining T_i by trial and then differentiating q/q_{Nu} with respect to $(T_\infty - T_w)$. Similar maxima were observed in the flat plate study of [7]; however, those reported here occur at larger $(T_\infty - T_w)$ and reductions in q/q_{Nu} with further increases in $(T_\infty - T_w)$ are less marked. This of course is due to enhancement of $\mathscr{G}$ under conditions of forced flow.

Steam (m_2)–*methanol* (m_1) *results*

For condensation of mixed vapors, the effects of $\rho_\infty u_\infty$, $\mathscr{B}$, R, and $T_\infty - T_w$, as discussed above, are further complicated by (i) the effects of composition $m_{1,u}$ on the physical property

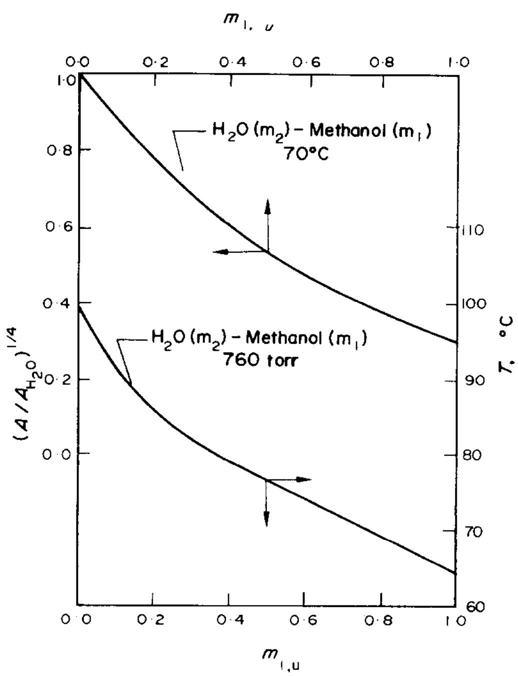

FIG. 8. Vapor–liquid equilibria and effects of $m_{1,u}$ on $A = k_l\rho_l\lambda/v_l$ for steam–methanol.

Table 1. Comparison of equations (29)–(31) *and* (35) *with numerical solutions; steam* (m_2)–*air* (m_1)

$T_\infty - T_w$	$m_{1,\infty}$	u_∞ (ft/s)	$\rho_\infty u_\infty$ (lb/ft²s)	$-\mathscr{B}$	Re	q/q_{Nu}	ε_q*	ε_g†	ε_τ‡
A. R = 0·75 in., P_∞ = 760 Torr									
40	0·01	10	0·369	0·914	5480	1·420	−0·75	1·2	−5·7
40	0·15	10	0·393	0·741	5260	0·648	0·80	4·1	4·9
40	0·01	1	0·0369	0·966	548	0·803	−0·31	3·1	−8·1
40	0·15	1	0·0393	0·775	526	0·252	−4·90	6·7	7·0
10	0·01	10	0·369	0·675	5480	1·310	0·21	−0·88	0·75
10	0·15	10	0·393	0·479	5260	0·555	3·2	3·3	5·8
10	0·01	1	0·0369	0·852	548	0·833	−0·58	−1·3	−6·1
10	0·15	1	0·0393	0·548	526	0·243	3·3	3·4	6·2
0·3	0·01	10	0·369	0·104	5480	0·636	0·84	3·5	2·0
0·3	0·15	10	0·393	0·392	5260	0·062	2·1	2·6	1·0
0·3	0·01	1	0·0369	0·187	548	0·367	1·9	3·0	2·4
0·3	0·15	1	0·0393	0·044	526	0·023	3·5	3·9	1·2
B. R = 0·75 in., P_∞ = 49 Torr									
40	0·01	100	0·286	0·938	5148	2·74	1·6	1·1	1·9
40	0·05	100	0·291	0·910	5060	1·81	3·2	2·5	1·1
40	0·15	100	0·304	0·796	4880	1·02	5·1	4·3	5·9
1	0·01	100	0·286	0·324	5148	1·85	1·7	2·6	3·8
1	0·05	100	0·291	0·257	5060	1·025	2·7	3·9	4·2
1	0·15	100	0·304	0·154	4880	0·363	0·31	4·4	3·7

C. P_∞ = 760 Torr, $T_\infty - T_w$ = 20°F, u = 10 ft/s, $m_{1,\infty}$ = 0·05

R (in.)	$\rho_\infty u_\infty$	$-\mathscr{B}$	Re	q/q_{Nu}	ε_q	ε_g	ε_τ
1·500	0·376	0·769	10,800	0·93	0·32	0·47	0·00
0·500	0·376	0·753	2,600	1·15	0·58	−0·31	0·54
0·325	0·376	0·750	2,700	1·22	0·64	−0·27	0·63
0·250	0·376	0·747	1·800	1·34	0·71	0·24	0·74

D. R = 0·75 in., $T_\infty - T_w$ = 20°F, u_∞ = 10 ft/s, $m_{1,\infty}$ = 0·05

T (°F)	$\rho_\infty u_\infty$	$-\mathscr{B}$	Re	q/q_{Nu}	ε_q	ε_g	ε_τ
212	0·387	0·756	5560	1·13	0·50	−0·36	0·40
180	0·208	0·793	3140	1·01	0·40	−0·42	0·05
150	0·108	0·824	1712	0·89	0·34	−0·40	−0·20
114	0·0441	0·858	756	0·76	0·43	−0·17	−0·37
80	0·0165	0·885	398	0·62	0·72	0·23	−0·34

* $\varepsilon_q = 100.(q/q_{Nu} - q/q_{Nu}|_{\text{equations (29), (30)}})/(q/q_{Nu})$.
† $\varepsilon_g = 100.(g - g|_{\text{equation (31)}})/g$.
‡ $\varepsilon_\tau = 100.(\tau_i - \tau_i|_{\text{equation (35)}})/\tau_i$.

group $A = k_l^3\rho_l\lambda/v_l$, and (ii) vapor–liquid equilibrium considerations. Since k_l, ρ_l, and $\lambda = m_{1,u}\lambda_1 + m_{2,u}\lambda_2$ decrease with increasing methanol concentration ($m_{1,u}$) and μ_l exhibits a strong maximum at $m_{1,u} \doteqdot 0{\cdot}5$, the ratio $(A/A_{H_2O})^{\frac{1}{4}}$ decreases sharply with increasing $m_{1,u}$ (Fig. 8). Furthermore, as condensation takes place, [more volatile] methanol accumulates at the s-surface ($m_{1,s} > m_{1,\infty}$) and T_i is reduced (see Fig. 8). Thus, $q/q_{Nu,H_2O}$ initially declines rapidly (Figs. 6 and 7) with increasing $m_{1,\infty}$. However, as $m_{1,\infty} \to 1$ the extent to which methanol can accumulate at the s-surface is constrained, $T_i - T_w \to T_\infty - T_w$, and minima in q/q_{Nu} occur. Of interest are the effects of u_∞ and $(T_\infty - T_w)$ on the locus of $q/q_{Nu}|_{\min}$. As illustrated in Figs. 6–7, $q/q_{Nu}|_{\min}$ shifts to the right with increasing u_∞ and $T_\infty - T_w$. This effect is due to enhancement of g, which serves to ameliorate the effects of net accumulation of [more volatile] methanol at the s-surface.

A simplified theory

Since equation (28) predicts, at least qualitatively, effects of the major problem parameters, the possibilities for a simplified theory are encouraging. If T_i is for the moment presumed known, the liquid-side problem is decoupled from that in the vapor phase provided an appropriate expression for vapor drag (τ_i) can be found. Formally,

$$q = q(T_i, \tau_i). \tag{29}$$

Further assuming that an adequate expression for g can be found, q alternatively can be written as

$$q \doteq -\lambda \mathscr{B} g(\mathscr{B}) \tag{30}$$

where $\mathscr{B}$ is known for given T_i. Thus equations (29) and (30) could in principle be solved simultaneously for the unknown T_i and, hence, q.

Following Acrivos [13], we assume that

$$g = [g_0^{\frac{3}{2}} + (-\mathscr{B} g_{-1})^{\frac{3}{2}}]^{\frac{2}{3}} \tag{31}$$

where g_{-1} is defined in equation (27) and g_0 is the conductance in the limit $\dot{m} \to 0$ [14]:

$$g_0 = 1{\cdot}15\, \rho_\infty u_\infty / R^{\frac{1}{2}} Sc^{0{\cdot}6}. \tag{32}$$

For boundary-layer flows undergoing strong suction, the asymptotic analogue of g_{-1} for shear is

$$\tau_{i,-1} = -\dot{m}(u_e - u_i) \tag{33}$$

whereas; that for $\dot{m} \to 0$ is [15]

$$\tau_{i,0} \doteq 4{\cdot}94\, \rho_\infty u_\infty^2 (x/R)/Re^{\frac{1}{2}},\ x \ll 1. \tag{34}$$

Paralleling the procedure for g, we take

$$\tau_i = [\tau_{i,0}^n + \tau_{i,-1}^n]^{1/n} \tag{35}$$

where, in the present situation, $n = 11/8$ proved to give a best fit to the true shear.

Equations (29) and (30) were solved for q/q_{Nu}, using equations (31) and (35) to predict g and τ_i. Typical results are summarized in Tables 1 and 2, where percentage errors in predicting q/q_{Nu}, g and τ_i are listed respectively as ε_q, ε_g and ε_τ. Considering the range of parameters involved $(-0{\cdot}966 \leqslant \mathscr{B} \leqslant -0{\cdot}044)$ and the contrasting

Table 2. Comparisons of equations (29)–(31) and (35) with numerical solutions steam (m_2)*-methanol* (m_1), $R = 0{\cdot}75$ *in.* $P_\infty = 760$ *Torr*

$T_\infty - T_w$	$m_{1,\infty}$	u_∞	$\rho_\infty u_\infty$	$-\mathscr{B}$	Re	q/q_{Nu}	ε_q	ε_g	ε_τ
40	0·90	10	0·658	0·728	10800	0·450	−1·6	0·68	−1·6
40	0·50	10	0·484	0·748	7340	0·477	−1·8	1·8	−2·5
40	0·10	10	0·386	0·916	5580	0·966	−3·9	−2·5	−6·7
20	0·90	100	6·58	0·527	108000	1·19	−0·44	1·7	2·0
20	0·50	100	4·84	0·497	73400	1·18	3·0	6·6	2·1
20	0·10	100	3·86	0·777	55800	2·58	−1·9	−0·09	−0·68
20	0·80	50	3·02	0·483	48400	0·744	−0·06	3·6	2·0
20	0·50	50	2·42	0·500	36600	0·835	3·3	6·5	2·1
20	0·10	50	1·98	0·777	28000	1·83	−1·9	−0·06	−0·68
20	0·70	10	0·556	0·466	8740	0·330	1·9	5·7	2·2
20	0·30	10	0·429	0·633	6340	0·549	1·4	4·8	1·6
20	0·70	1	0·056	0·614	874	0·168	2·0	5·1	2·3
20	0·30	1	0·043	0·744	634	0·260	3·8	7·1	2·6
10	0·70	10	0·556	0·245	8740	0·255	3·7	8·2	2·6
10	0·30	10	0·429	0·438	6340	0·499	3·7	6·6	3·2

natures of the noncondensable versus binary condensation problems, the results indicate that the method may safely apply to other systems. The method is of further practical value since it provides an accurate starting point for predicting heat transfer in the non-similar region between stagnation and separation. Since upwards of 80 per cent of the total heat transfer typically occurs in this region, the feasibility of predicting the effects of forced flow and noncondensables on overall heat transfer rates for, at least, the forward tubes in commercial condensers appears promising.

REFERENCES

1. W. NUSSELT, Die oberflachen-kondensation des wasserdampfes, *Z. Ver. Deutsch. Ing.* **60**, 569–575 (1916).
2. L. A. BROMLEY, Effect of heat capacity on condensate in condensing, *Ind. Engng Chem.* **44**, 2966–2969 (1952).
3. W. M. ROHSENOW, Heat transfer and temperature distribution in laminar-film condensation, *J. Heat Transfer* **78**, 1645–1648 (1956).
4. E. M. SPARROW and J. L. GREGG, Laminar condensation heat transfer on a horizontal cylinder, *J. Heat Transfer* **81**, 291–296 (1959).
5. I. G. SHEKRILADZE and V. E. GOMELAURI, Theoretical study of laminar film condensation of a flowing vapor, *Int. J. Heat Mass Transfer* **9**, 581–591 (1966).
6. V. E. DENNY and A. F. MILLS, Laminar film condensation of a flowing vapor on a horizontal cylinder at normal gravity, *J. Heat Transfer* **91**, 495–501 (1969).
7. W. J. MINKOWYCZ and E. M. SPARROW, Condensation heat transfer in the presence of noncondensables, interfacial resistance, superheating, variable properties, and diffusion, *Int. J. Heat Mass Transfer* **9**, 1125–1144 (1966).
8. V. E. DENNY, A. F. MILLS and V. J. JUSIONIS, Laminar film condensation from a steam–air mixture undergoing forced flow down a vertical surface, *J. Heat Transfer* **93**, 297–304 (1971).
9. D. F. OTHMER, The condensation of steam, *Ind. Engng Chem.* **21**, 577–583 (1929).
10. E. M. SPARROW and E. MARSCHALL, Binary, gravity-flow film condensation, *J. Heat Transfer* **91**, 205–211 (1969).
11. V. J. JUSIONIS, Effects of noncondensables, forced flow, and variable properties on film condensation of pure and binary vapors, Ph.D. dissertation, University of California, Los Angeles (1971).
12. Y. KNOBEL, Laminar film condensation on a horizontal cylinder, M.S. thesis, University of California, Los Angles (1969).
13. A. ACRIVOS, Mass transfer in laminar-boundary-layer flows with finite interfacial velocities, *A.I.Ch.E. Jl* **6**, 410–414 (1960).
14. W. M. KAYS, *Convective Heat and Mass Transfer*. McGraw-Hill, New York (1966).
15. H. SCHLICHTING, *Boundary Layer Theory*. McGraw-Hill, New York (1960).

EFFETS DE LA VITESSE, DES INCONDENSABLES ET DES PROPRIETES VARIABLES SUR LA CONDENSATION EN FILM DES VAPEURS PURES OU BINAIRES AU POINT D'ARRET AMONT D'UN CYLINDRE HORIZONTAL

Résumé—On présente une étude analytique des effets de la vitesse, des gaz incondensables et des propriétés thermophysiques variables sur la condensation laminaire en film des vapeurs pures ou binaires au point d'arrêt amont d'un cylindre horizontal. Les résultats du transfert thermique par condensation sont obtenus pour une gamme étendue de paramètres incluant la vitesse moyenne amont ($u_\infty = 0{,}3$–30 m/s), la pression de saturation ($P_\infty = 49$–760 Torr); la différence de température entre fluide au loin et paroi ($T_\infty - T_W = 0{,}166$–$22{,}3$°C), la fraction massique de gaz non condensable ($m_{1,\infty} = 0{,}01$–$0{,}15$) et le rayon du cylindre ($R = 0{,}635$–$3{,}81$ cm). Comme prévu les effets néfastes d'un gaz non condensable sur q/q_{Nu} (q_{Nu} est la solution classique de Nusselt pour la vapeur pure) dans les conditions de repos sont beaucoup moins sévères avec un écoulement forcé. (Pour des mélanges vapeur d'eau–air avec $0{,}01 < m_{1,\infty} < 0{,}15$, q/q_{Nu} double approximativement quand u_∞ croit de 0,3 à 3,3 m s). Comme pour les résultats de Minkowycz et Sparrow pour la plaque plane, q/q_{Nu} passe par un maximum quand $T_\infty - T_W$ augmente; ici, le maximum se produit pour une valeur plus élevée de $T_\infty - T_W$ et est plus prononcé. Pour une condensation binaire en film de mélanges vapeur d'eau–methanol, on trouve que q/q_{Nu} (q_{Nu} est la solution classique de Nusselt pour la vapeur pure) décroît fortement quand la concentration de méthanol (plus volatil) augmente; l'effet est comparable à celui d'un gaz incondensable. Guidé par les résultats numériques, on développe une théorie simplifiée qui est en bon accord avec les conductances thermiques et massiques.

EINFLÜSSE DER ZWANGSKONVEKTION, NICHT-KONDENSIERBARER STOFFE UND VERÄNDERLICHER STOFFWERTE AUF DIE FILMKONDENSATION VON REINEN UND BINÄREN DÄMPFEN AM VORDEREN STAUPUNKT EINES HORIZONTALEN ZYLINDERS

Zusammenfassung—Es wird eine analytische Untersuchung der Einflüsse der Zwangskonvektion, nicht kondensierbaren Gases und der veränderlichen thermophysikalischen Stoffwerte auf die laminare Filmkondensation reiner und binärer Dämpfe am vorderen Staupunkt eines horizontalen Zylinders angestellt. Ergebnisse des Wärmeübergangs bei der Kondensation wurden für einen grossen Parameterbereich errechnet. Darin sind eingeschlossen die Anströmgeschwindigkeit (u_∞ = 0,3–30 m/s), der Sättigungsdruck (P_∞ = 49–760 Torr), die Temperaturdifferenz zwischen Wand und anströmendem Fluid ($T_\infty - T_W$ = 0,16–22 K), Massenanteil des nichtkondensierbaren Gases ($m_{1,\infty}$ = 0,01–0,15) und der Zylinderradius (R = 0,65–3,75 cm). Wie erwartet, sind die schädlichen Einflüsse des nicht kondensierbaren Gases auf q/q_{Nu} (q_{Nu} ist die klassische Nusseltlösung für reinen Dampf) ohne Anströmung wesentlich ausgeprägter als bei Zwangskonvektion. (Bei Dampf-Luft-Gemischen, mit $0{,}01 \leqslant m_{1\infty} \leqslant 0{,}15$ verdoppelt sich q/q_{Nu} ungefähr, wenn u_∞ von 0,3 bis 30 m/s steigt). Was für die Versuche von Minkowycz und Sparrow an der ebenen Platte galt, trifft auch hier zu: q/q_{Nu} durchläuft ein Maximum mit steigendem $T_\infty - T_W$; hier liegt das Maximum jedoch bei höheren $T_\infty - T_W$ und ist ausgeprägter. Bei der Filmkondensation des binären Gemisches Dampf-Methanol ergibt sich, dass q/q_{Nu} stark abnimmt mit zunehmender Freistromkonzentration des (flüchtigen) Methanols; der Einfluss ist ähnlich dem des nicht kondensierbaren Gases. Durch numerische Ergebnisse geleitet wird eine vereinfachende Theorie entwickelt, die in guter Übereinstimmung mit den Wärme- und Stoffübergangswiderständen ist.

ИССЛЕДОВАНИЕ ВЛИЯНИЯ ВЫНУЖДЕННОГО ТЕЧЕНИЯ, НЕКОНДЕНСИРУЮЩИХСЯ ВЕЩЕСТВ И ПЕРЕМЕННЫХ СВОЙСТВ НА ПЛЕНОЧНУЮ КОНДЕНСАЦИЮ ЧИСТЫХ И БИНАРНЫХ ПАРОВ В ПЕРЕДНЕЙ КРИТИЧЕСКОЙ ТОЧКЕ ГОРИЗОНТАЛЬНОГО ЦИЛИНДРА

Аннотация—Проведено аналитическое исследование влияния неконденсирующегося газа и переменных теплофизических свойств на пленочную конденсацию чистых и бинарных паров в передней критической точке горизонтального цилиндра при ламинарном вынужденном обтекании. Результаты по теплообмену при конденсации получены для широкого диапазона параметров, а именно : скорости основного потока (u_∞ = 1–100 фт/сек), давления насыщения (P_∞ = 49–760 торр), разности температур основного потока и стенки ($T_\infty - T_w$ = 0,3–40°F), весовой концентрации неконденсирующегося газа ($m_{l,\infty}$ = 0,01–0,15) и радиуса цилиндра (R = 0,25–1,5 дюйма). Как и предполагалось, отрицательное в уловиях отсутствия движения воздействие неконденсирующегося газа на величину q/q_{Nu}, где q_{Nu} — результат классического решения Нуссельта для чистого пара, значительно менее сказывается при вынужденном течении. При $0{,}01 \leq m_{l,\infty} \leq 0{,}15$ для паровоздушных смесей q/q_{Nu} возрастает приблизительно в 2 раза при увеличении u_∞ от 1 до 10 фт/сек. Аналогично результатам Минковича и Спэрроу для плоской пластины q/q_{Nu} проходит через максимум по мере роста $T_\infty - T_w$. В данной работе максимум более четко выражен и имеет место при больших значениях разности $T_\infty - T_w$. Установлено, что при бинарной пленочной конденсации смесей водяной пар-метанол величина q/q_{Nu}, где q_{Nu}-результат классического решения Нуссельта для чистого пара, резко снижается при увеличении объемной концентрации более летучего компонента (метанола). Этот эффект подобен влиянию неконденсирующегося газа. На основании численных решений разработана весьма удовлетворительная упрощенная теория.